Monatsh Chem (2010) 141:395–400
DOI 10.1007/s00706-010-0279-3

ORIGINAL PAPER

Two new Co(II) complexes of benzimidazole: synthesis, characterization, and electrocatalysis

**Rui Rui Zhuang · Fang Fang Jian ·
Ke Fei Wang**

Received: 9 October 2009 / Accepted: 23 February 2010 / Published online: 18 March 2010

Abstract Two new complexes, [Co(C_3H_7-bim)$_2$Br$_2$] and [Co(C_5H_{11}-bim)$_2$Br$_2$], have been synthesized and the structures characterized by X-ray crystallography, IR spectroscopy, and elemental analysis. The cobalt atoms of the two complexes both adopt distorted tetrahedral geometry. The electrochemical behavior of and electrocatalysis by the propyl complex bulk-modified carbon paste electrode have been studied by cyclic voltammetry. It has good electrocatalytic activity toward reduction of trichloroacetic acid (TCA) and bromate. The detection limit and the sensitivity are 0.01 μM and 60.93 μA μM^{-1} for TCA detection, and 0.02 μM and 43.94 μA μM^{-1} for bromate detection. This modified electrode has good reproducibility, high stability, low detection limit, technical simplicity, and possibility of rapid preparation, which is important for practical application.

Keywords Cobalt complexes · Crystal structure · Electrochemistry · Cyclic voltammetry

Introduction

The significant contemporary interest in organic–inorganic hybrid materials reflects both the fundamental chemistry of the rational design of complex materials and practical applications to fields as diverse as catalysis [1], optical materials [2, 3], membranes [4–6], and sorption [7, 8]. In these materials, transition metal complexes with diverse structural arrangements not only serve as charge-compensating units but also modify the wide-ranging properties, for example magnetic and optical properties, electronic conductivities, and electrocatalysis [9, 10]. Recently, great efforts have been directed toward the study of Cu(II) complexes incorporating pyridine, thioether, imidazole, and imine donors, which not only stem from their fascinating structures but also from their potential applications as new materials [11–16]. The electrochemistry and electrocatalysis of copper complexes with various different ligands have been investigated by several groups [17–19]. Wang et al. [20] investigated electrocatalytic activity toward the reduction of bromate, nitrite, and hydrogen peroxide of a copper-complex bulk-modified carbon paste electrode (CPE). Jiang et al. [21] studied electrocatalysis for trichloroacetic acid (TCA) reduction of a binuclear cobalt phthalocyaninehexasulfonate-surfactant film-modified electrode.

Interest in exploring benzimidazole derivatives and their metal complexes has continually increased, because many of these materials may serve as models which mimic both the structure and reactivity of metal ion sites in complex biological systems [22–29]. Xia et al. [24] studied the synthesis, structures, and magnetic properties of Co(II) complexes based on 2-(*N*-pyridyl)benzimidazole. Sánchez-Guadarrama et al. [25] studied the cytotoxic activity, X-ray crystal structures, and spectroscopic characterization of cobalt(II), copper(II), and zinc(II) coordination compounds with 2-substituted benzimidazoles. López-Sandoval et al. [26] reported the synthesis, structures, and biological activity of Co(II) complexes with 2-benzimidazole derivatives. Despite all this work, to our best knowledge, study of the electrochemistry and electrocatalysis of cobalt complexes containing benzimidazole is less reported [25–29]. This paper work reports the synthesis and characterization of

R. R. Zhuang · F. F. Jian (✉) · K. F. Wang
New Materials and Function Coordination Chemistry Laboratory, Qingdao University of Science and Technology, Qingdao, People's Republic of China
e-mail: ffj2003@163169.net

two new Co(II) complexes, [Co(C_3H_7-bim)$_2$Br$_2$] (**1**) and [Co(C_5H_{11}-bim)$_2$Br$_2$] (**2**) (bim = benzimidazole). The electrochemical behavior of and electrocatalysis by the title complex [Co(C_3H_7-bim)$_2$Br$_2$] bulk-modified carbon paste electrode (**1**-CPE) have been studied by cyclic voltammetry. This modified electrode has excellent electrocatalytic activity toward the reduction of TCA and bromate, and possible mechanisms are proposed.

Results and discussion

Crystal structure of the title complexes

Crystal data and structure refinement of two title complexes are listed in Table 1. The molecular structure of [Co(C_3H_7-bim)$_2$Br$_2$] (**1**) with the atomic numbering scheme is shown in Fig. 1. The structure of the title complex **1** contains a pair of independent, unconnected [Co(C_3H_7-bim)$_2$Br$_2$] asymmetric units. The cobalt atom adopts distorted tetrahedral geometry involving two bromine atoms and two nitrogen atoms from two 1-propyl-1*H*-benzo[*d*]imidazole ligands. The Co–Br [Co(1)–Br(1) 2.38(2) and Co(1)–Br(2) 2.384(2) Å] and Co–N [Co(1)–N(4) 2.014(7) and Co(1)–N(2) 2.027(6) Å] bond lengths are comparable with those found in similar complexes [25, 26]. The angles around the Co center are N(4)–Co(1)–N(2) 114.2(2)°, N(4)–Co(1)–Br(1) 105.2(2)°, N(2)–Co(1)–Br(1) 111.9(2)°, N(4)–Co(1)–Br(2) 105.5(2)°, N(2)–Co(1)–Br(2) 104.4(2)°, and Br(1)–Co(1)–Br(2) 115.80(6)°. These values are consistent with similar structures reported earlier [25, 26]. There are two types of π–π stacking interactions between the imidazole and phenyl rings and the center-to-center distances both are 3.9664 Å. The shortest interplanar distances are 3.626 and 3.657 Å, respectively. There are also two types of π–π stacking interactions between phenyl ring and phenyl ring and the center-to-center distances are 3.7295 and 3.7611 Å. The shortest interplanar distances above are 3.638 and 3.532 Å, respectively. There are two types of C–H···π stacking interactions. The distance of C(16) to the plane [C(5)–C(6)–C(7)–C(8)–C(9)–C(10)] is 3.7419 Å. The distance of C(21) to the plane [C(25)–C(26)–C(27)–C(28)–C(29)–C(30)] is 3.6136 Å. In the solid state, all these intermolecular interactions stabilize the crystal structure.

The molecular structure of the title complex **2** with the atomic numbering scheme is shown in Fig. 2. The cobalt atom

Table 1 Crystal data and structure refinement for the two title complexes

Empirical formula	$C_{40}H_{48}Br_4Co_2N_8$	$C_{24}H_{32}Br_2CoN_4$
Formula weight	1,078.36	595.29
Temperature (K)	293(2)	293(2)
Wavelength (Å)	0.71073	0.71073
Crystal system, space group	Triclinic, $P\bar{1}$	Trigonal, $R\,\bar{3}$
Unit cell dimensions		
a (Å)	10.153(2)	27.569(4)
b (Å)	10.732(2)	27.569(4)
c (Å)	23.342(5)	19.701(4)
α (°)	76.96(3)	90
β (°)	81.82(3)	90
γ (°)	66.40(3)	120
Volume (Å^3)	2,266.8(8)	12,968(4)
Z, Calculated density (g cm^{-3})	2, 1.580	18, 1.372
Absorption coefficient (mm^{-1})	4.294	3.385
F(000)	1,076	5,418
Theta range for data collection (°)	3.01–27.48	3.06–27.48
Limiting indices	$-13 \le h \le 10$, $-13 \le k \le 13$, $-30 \le l \le 29$	$-35 \le h \le 35$, $-33 \le k \le 35$, $-25 \le l \le 25$
Reflections collected/unique	21,543/10,051 [$R_{int} = 0.0872$]	40,824/6,602 [$R_{int} = 0.1188$]
Completeness to θ (%)	96.7	99.8
Data/restraints/parameters	10,051/2/488	6,602/4/281
Goodness-of-fit on F^2	1.085	0.913
Final *R* indices [$I > 2\sigma(I)$]	$R_1 = 0.0818$, $wR_2 = 0.2001$	$R_1 = 0.0610$, $wR_2 = 0.1565$
R indices (all data)	$R_1 = 0.1413$, $wR_2 = 0.2856$	$R_1 = 0.1657$, $wR_2 = 0.2077$
Largest difference peak and hole (*e* Å^{-3})	1.269 and −1.497	0.441 and −0.454

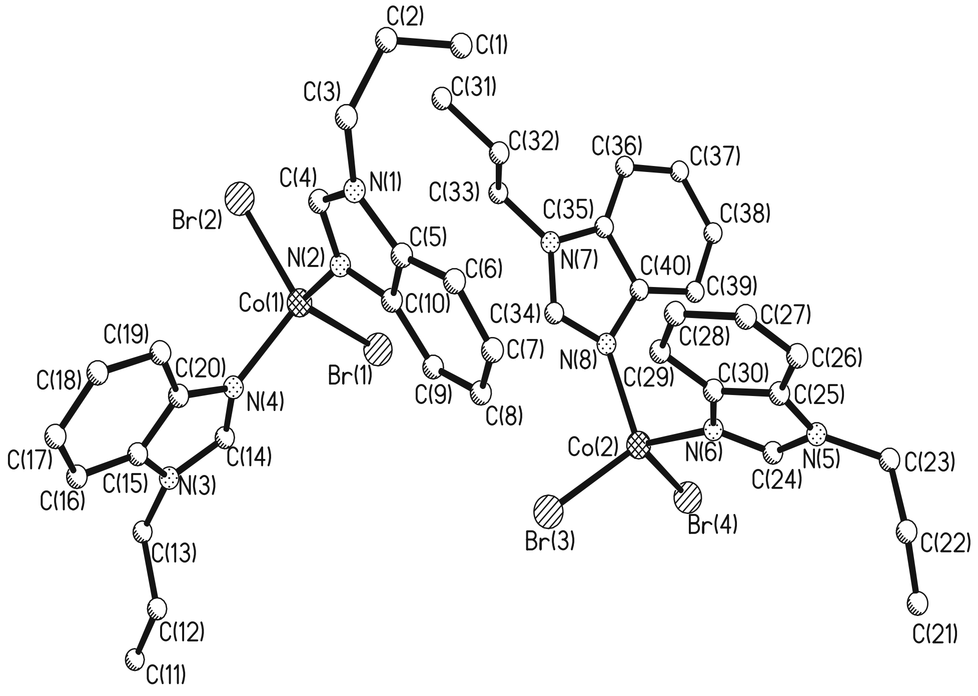

Fig. 1 The molecular structure of [Co(C_3H_7-bim)$_2$Br$_2$] (**1**) showing the atom labeling scheme

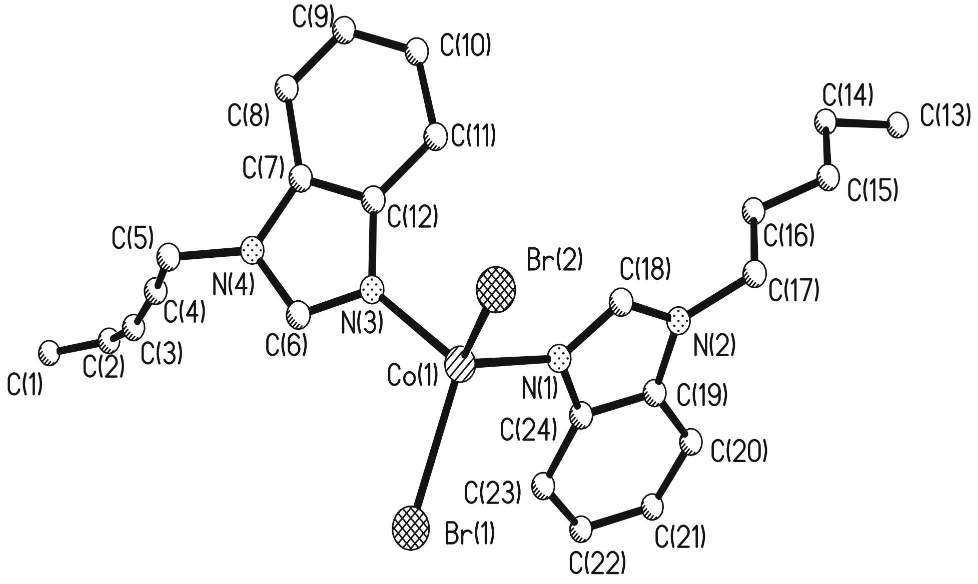

Fig. 2 The molecular structure of [Co(C_5H_{11}-bim)$_2$Br$_2$] (**2**) showing the atom labeling scheme

adopts a distorted tetrahedral geometry involving two bromine atoms and two nitrogen atoms from two 1-amyl-1*H*-benzo[*d*]imidazole ligands. The space group of the title complex **2** is not identical with that of the title complex **1**. The bond lengths and bond angles are similar to those of **1**. There are three types of π–π stacking interactions between the imidazole and phenyl rings and the center-to-center distance is in the range 3.5225–3.7745 Å. The shortest interplanar distances are in the range 3.405–3.432 Å. There are two types of π–π stacking interactions between phenyl ring and phenyl ring and the center-to-center distances are 3.5742 and 3.9505 Å. The shortest interplanar distances above are 3.393 and 3.448 Å, respectively. There is also one type of π–π stacking interaction between imidazole ring and imidazole ring and the center-to-center distance is 3.7745 Å. The shortest interplanar distance is 3.343 Å. In the solid state, all these intermolecular interactions stabilize the crystal structure.

*Electrochemical behavior of **1**-CPE*

The electrochemical behavior of **1**-CPE was investigated by cyclic voltammetry in aqueous solution. We chose a 0.1 M aqueous KCl solution, 0.1 M, pH 7.0, Britton–Robinson (B-R) buffer solution, and 0.1 M, pH 7.0, phosphate buffer solution

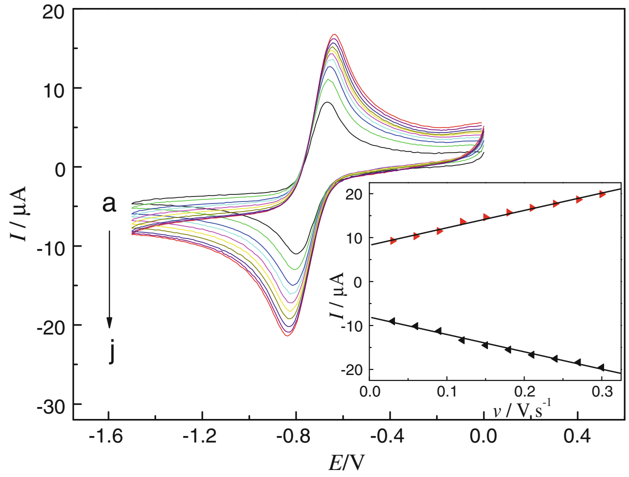

Fig. 3 CVs of **1**-CPE in 0.1 M, pH 6.1, B-R buffer solution. Curves *a–j* correspond to the scan rates 0.03, 0.06, 0.09, 0.12, 0.15, 0.18, 0.21, 0.24, 0.27, and 0.30 V s^{-1}, respectively. *Inset*: plot of peak current versus scan rate

as the supporting electrolyte solutions. It was found that the modified electrode in B-R buffer solution showed strong current response and symmetric peak shape. We then investigated the electrochemical behavior of the modified CPE in the pH range 4.0 to 8.0 in B-R buffer solution and found that the electrochemical signal was relatively stable at pH 6.1. Therefore, we studied the electrochemical behavior and electrocatalytic properties in 0.1 M, pH 6.1, B-R buffer solution.

The cyclic voltammograms (CVs) of **1**-CPE are presented in Fig. 3. When the scan rate was 0.03 V s^{-1}, the curve a had two redox peaks at −0.808 and −0.675 V, with the formal potential ($E^{0'}$) at −0.741 V, corresponding to the electrochemical process Co(II)/Co(I). The separation of the cathodic and anodic peak potential, $\Delta E = 0.133$ V, $i_{pc}/i_{pa} = 1.06$, indicated that the electrochemical behavior of the title complex on the electrode was quasi reversible.

The effect of scan rate on the electrochemical behavior of **1**-CPE can be seen from Fig. 3. When the scan rate was varied from 0.03 to 0.30 V s^{-1}, the peak potentials changed gradually: with increasing scan rate the cathodic peak potentials shifted to the negative direction and the corresponding anodic peak potentials shifted to the positive direction. The plot of peak current versus the scan rate is shown in the inset of Fig. 3. The anodic and cathodic currents are proportional to the scan rate, suggesting that the redox process is confined to the surface.

*Electrocatalytic activity of **1**-CPE*

Electrocatalytic reduction of TCA

Organohalides are found as pollutants of the environment. TCA is formed during water chlorination. Electrochemical oxidation or reduction is an effective measure for dealing with pollutants of the environment [21]. Some insoluble metal complexes containing redox mediators can be used for electrocatalysis. The electrocatalytic activity of **1**-CPE toward TCA is shown in Fig. 4. On addition of TCA to the solution (curves a–e), the oxidation and reduction peak potentials did not obviously change, there was dramatic enhancement of the cathodic peak current, and the anodic peak current decreased. When the concentration of TCA added was 0.20 μM, the maximum value of the reduction peak current was obtained, and the value of the oxidation peak current was almost reduced to zero, which indicated a strong catalytic effect. The possible reaction processes could be described by use of the following equations [21, 30]:

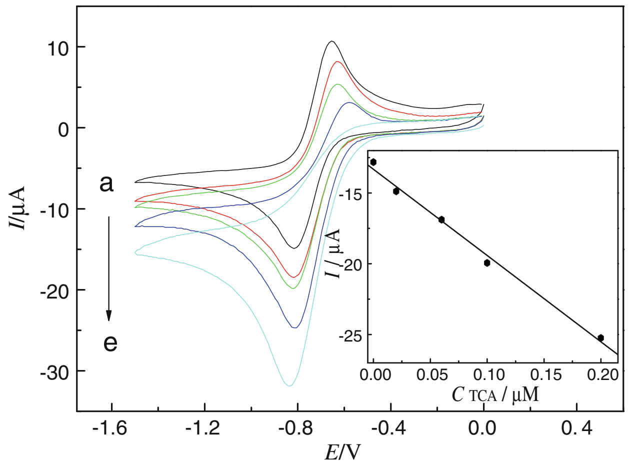

Fig. 4 CVs of **1**-CPE in 0.1 M, pH 6.1, B-R buffer solution containing (*a–e*) 0, 0.02, 0.06, 0.10, and 0.20 μM TCA, with a scan rate of 0.10 V s^{-1}. *Inset*: plot of cathodic peak current versus TCA concentration

$$\mathrm{Co(II)} + e^{-} \leftrightarrow \mathrm{Co(I)}$$

$$2\mathrm{Co(I)} + \mathrm{CCl_3COOH} + \mathrm{H^+} \leftrightarrow 2\mathrm{Co(II)} + \mathrm{CHCl_2COOH} + \mathrm{Cl^-}$$

The inset of Fig. 4 shows that the catalytic current varies linearly with TCA concentration in the range 0.02–0.20 μM. The linear regression equation is $I_{pc}(\mu A) = -60.93C$ (μM) − 13.32 with a correlation coefficient of 0.996. The detection limit (signal to-noise ratio = 3) and sensitivity are 0.01 μM and 60.93 μA μM^{-1}, respectively.

Electrocatalytic reduction of bromate

Bromate is a disinfectant by-product contaminant found in drinking water, and is formed during the ozonation of source water containing bromide. The overpotential for bromate reduction is high and, therefore, an efficient electrocatalyst would be beneficial [20]. However, the reduction of bromate can readily be catalyzed by **1**-CPE in

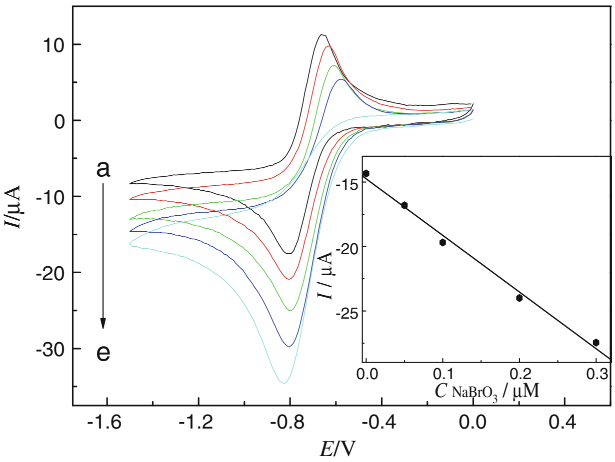

Fig. 5 CVs of **1**-CPE in 0.1 M, pH 6.1, B-R buffer solution containing (*a–e*) 0, 0.05, 0.10, 0.20, and 0.30 μM bromate, with a scan rate of 0.10 V s^{-1}. *Inset*: plot of cathodic peak current versus bromate concentration

0.1 M, pH 6.1, B-R buffer solution. As shown in curves a–e in Fig. 5, on addition of bromate the peak potentials had little change, and the reduction peak current increased while the corresponding oxidation peak decreased. When the concentration of bromate added was 0.30 μM, the maximum value of the reduction peak current was obtained, and the value of the oxidation peak current was almost reduced to zero, indicating that **1**-CPE had excellent electrocatalytic activity in the reduction of bromate. The possible reaction processes could be described in the following equations [20, 30]:

$$\mathrm{Co(II)} + e^{-} \leftrightarrow \mathrm{Co(I)}$$

$$6\mathrm{Co(I)} + \mathrm{BrO_3^-} + 6\mathrm{H^+} \leftrightarrow 6\mathrm{Co(II)} + \mathrm{Br^-} + 3\mathrm{H_2O}$$

The inset of Fig. 5 shows that the catalytic current varies linearly with bromate concentration in the range 0.05–0.30 μM. The linear regression equation is $I_{pc}(\mu A) = -43.94C(\mu M) - 14.75$ with a correlation coefficient of 0.996. The detection limit (signal-to-noise ratio = 3) and the sensitivity are 0.02 μM and 43.94 μA μM^{-1}, respectively. Comparing the performances of the different electrochemical sensors for bromate, this detection limit is much lower than earlier reports (0.1 μM [10], 0.036 μM [13], and 0.6 μM [2]) in which other modified electrodes were used.

Compared with other modified film electrodes, the title complex-modified electrode showed high stability. In our experiment, after the electrocatalytic reaction **1**-CPE was investigated in buffer solution under the same condition as shown in Fig. 3, and we found that the peak potentials and peak currents had no obvious change, which suggested that no new materials appeared. This indicated that the title complex was still stable and acted as catalyst during the reactions. When the potential was maintained in the same range, it was stable over 100 cycles at a scan rate of 0.10 V s^{-1} and the current response remained almost unchanged. When the bulk-modified CPE was stored at room temperature for at least two months, the current response decreased by 2.1% only.

Conclusions

In summary, two new complexes, $[\mathrm{Co(C_3H_7\text{-}bim)_2Cl_2}]$ and $[\mathrm{Co(C_5H_{11}\text{-}bim)_2Cl_2}]$, were synthesized and the structures were characterized. The electrochemical behavior and electrocatalysis of **1**-CPE have been investigated. This modified electrode has excellent electrocatalytic activity in the reduction of TCA and bromate, and the results are reproducible with a lower detection limit than mentioned in earlier reports. They may, therefore, be suitable for quantitative analysis of environmentally hazardous materials. The advantages of the bulk-modified **1**-CPE are stability, excellent catalytic activity, low detection limit, and simplicity of preparation compared with other methods; these advantages seem promising for construction of chemical and biosensors.

Experimental

Chemicals and measurements

All chemicals were analytical reagent-grade and used without further purification. Elemental analyses were performed with a Perkin–Elmer (USA) 1400C analyzer, and results agreed with calculated values. Infrared spectra in the 4,000–400 cm^{-1} range were recorded on a Nicolet 170SX spectrometer (USA) using pressed KBr disks. Crystal structure was determination by X-ray diffraction on a Bruker–Nonius diffractometer with Kappa geometry attached to an APEXII-CCD detector (Bruker, Germany). Electrochemical measurements were performed with an Autolab PGSTAT-30 digital potentiostat/galvanostat (EcoChemie, Utrecht, The Netherlands). A three-electrode cell was used in the experiments. The working electrode was a modified CPE. The counter-electrode was a platinum wire. The reference electrode was Ag|AgCl, KCl (1 M); all potentials reported in this work were measured relative to this electrode (236.3 mV/SHE at 25 °C). Britton–Robinson (B-R) buffer solution (0.1 M, pH 6.1) was used as the supporting electrolyte. All solutions were deaerated with pure nitrogen for 30 min and kept under a nitrogen atmosphere during the experiments. All measurements were performed at room temperature (25 ± 2 °C).

Dibromobis(1-propyl-1H-benzimidazol-N3)cobalt (**1**, $C_{20}H_{24}Br_2CoN_4$)

$[\mathrm{Co(C_3H_7\text{-}bim)_2Br_2}]$ (**1**) was synthesized by dissolving 219 mg cobaltous bromide (1 mmol) and 321 mg 1-propyl-1

H-benzo[*d*]imidazole (2 mmol) in 50 cm^3 ethanol and stirring for 2 h. The resulting blue precipitate was collected by filtration. Recrystallization from acetonitrile gave a yield of 76%. IR: $\bar{\nu} = 3{,}058, 2{,}952$, and 2,879 (C–H), 1,296 (C–N) cm^{-1}.

Dibromobis(1-pentyl-1H-benzimidazol-N3)cobalt (**2**, $C_{24}H_{32}Br_2CoN_4$)

$[Co(C_5H_{11}\text{-bim})_2Br_2]$ (**2**) was prepared similarly to **1**.

*X-ray analysis of **1** and **2***

X-ray diffraction was conducted at 20 °C using MoK_α radiation ($\lambda = 0.71073$ Å) with a graphite monochromator. The structures of the title complexes were solved by direct methods and refined by least squares on F^2_{obs} by using the *SHELXTL* software package [31]. All non-hydrogen atoms were refined anisotropically, and the hydrogen atoms were placed in calculated positions and allowed to ride on their parent atoms. The molecular graphics were plotted using *SHELXTL*. Atomic scattering factors and anomalous dispersion corrections were taken from the International Tables for X-ray Crystallography [32]. Crystallographic data of the structural analysis have been deposited at the Cambridge Crystallographic Data Centre, CCDC reference numbers 748738 and 741423. Copies of this information can be obtained free of charge from The Director, 12 Union Road, Cambridge, CB2 1EZ, UK (fax: +44-1223-336033; e-mail: deposit@ccdc.cam.ac.uk or http://www.ccdc.cam.ac.uk).

*Preparation of **1**-CPE*

The traditional CPE was prepared by hand-mixing graphite powder with paraffin oil in the ratio 70:30 (*w*/*w*) in an agate mortar. The modified CPE was fabricated as follows: 0.3 g graphite powder and 0.03 g title complex **1** in the ratio 10:1 (*w*/*w*) were mixed and ground together with an agate mortar and pestle for about 30 min to achieve an even, dry mixture. Paraffin oil (0.1 cm^3) was added to the mixture, which was stirred with a glass rod. The homogenized mixture was then used to fill a glass tube (3 mm inner diameter) to a depth of 0.8 cm. Electrical contact was established with a copper rod, and the surface of **1**-CPE was polished on a piece of weighing paper until it had a shiny surface.

Different ratios of graphite powder to title complex **1** were investigated to determine the optimum preparation conditions. We investigated the graphite powder and the title complex in the ratios 20:1, 14:1, 10:1, 8:1, and 5:1 (*w*/*w*), and found the optimum was 10:1. When the amount of the title complex was too little or too large, the electrochemical signal was too weak.

Acknowledgments This work was supported by the Natural Science Foundation of Shandong Province (No.Z2007B01), People's Republic of China.

References

1. Salimi A, Mamkhezri H, Mohebbi S (2006) Electrochem Commun 8:688
2. Salimi A, Mamkhezri H, Hallaj R, Zandi S (2007) Electrochim Acta 52:6097
3. Joshi PP, Merchant SA, Wang Y, Schmidtko DW (2005) Anal Chem 77:3183
4. Antiochia R, Gorton L (2007) Biosens Bioelectron 22:2611
5. Timur S, Anik U, Odaci D, Gorton L (2007) Electrochem Commun 9:1810
6. Wang Y, Joshi PP, Hobbs KL, Johnson MB, Schmidtko DW (2006) Langmuir 22:9776
7. Kim EH, Kim DI, Lee HS, Na HG, Byun JC, Choi JH, Park YC (2007) Polyhedron 26:85
8. Balamurugan R, Palaniandavar M, Halcrow MA (2006) Polyhedron 25:1077
9. Gao GG, Xu L, Wang WJ, An WJ, Qiu YF, Wang ZQ, Wang EB (2005) J Phys Chem B 109:8948
10. Salimi A, Alizadeh V, Hadadzadeh H (2004) Electroanalysis 16:1984
11. Cheung KC, Wong WL, Ma DL, Lai TS, Wong KY (2007) Coord Chem Rev 251:2367
12. Bressan M, Celli N, Dalessandro N, Liberatore L, Morvillo A, Onucci LT (2000) J Organomet Chem 594:416
13. Salimi A, Kavosi B, Babaei A, Hallaj R (2008) Anal Chim Acta 618:43
14. Laurent R, Claire CC, Jacqueline C, René T (2007) J Electroanal Chem 603:260
15. Markovic NM, Ross PN (1994) J Electrochem Soc 141:2590
16. Lee CK, Striebel KA, McLarnon FR, Cairns EJ (1997) J Electrochem Soc 144:3801
17. Kulesza PJ, Faulkner LR (1989) J Electroanal Chem 259:81
18. Kulesza PJ, Roslonek G, Faulkner LR (1990) J Electroanal Chem 280:233
19. Chen SM (1998) J Electroanal Chem 457:23
20. Wang XL, Zhao HY, Lin HY, Liu GC, Fang JN, Chen BK (2008) Electroanalysis 20:1055
21. Jiang XE, Guo LP, Du XG (2003) Talanta 61:247
22. Crane JD, Sinn E, Tann B (1999) Polyhedron 18:1527
23. Liu Z, Chen Y, Liu P, Wang J, Huang MH (2005) J Solid State Chem 178:2306
24. Xia CK, Lu CZ, Yuan DQ, Zhang QZ, Wu XY, Zhang JJ, Wu DM (2007) J Mol Struct 831:195
25. Sánchez-Guadarrama O, López-Sandoval H, Sánchez-Bartéz F, Gracia-Mora I, Höpfl H, Barba-Behrens NJ (2009) J Inorg Biochem 103:1204
26. López-Sandoval H, Londoño-Lemos ME, Garza-Velasco R, Poblano-Meléndez I, Granada-Macías P, Gracia-Mora I, Barba-Behrens N (2008) J Inorg Biochem 102:1267
27. Tarte NH, Woo SI, Cui LQ, Gong YD, Hwang YH (2008) J Organomet Chem 693:729
28. García FJB, García AB, Giles FL, Rogado MAM, Zahínos EV (2005) Polyhedron 24:1764
29. Wang SX, Yu SY, Luo QH (1994) Transit Metal Chem 19:205
30. Li YX, Lin XQ, Jiang CM (2006) Electroanalysis 18:2085
31. Sheldrick GM (2000) SHELXTL 6.10. Bruker Analytical Instrumentation, Madison
32. Wilson AJ (1992) International Table for X-ray Crystallography, V. C. Kluwer Academic Publishers, Dordrecht